

<https://doi.org/10.31288/oftalmolzh202533544>

***In vitro* and *in vivo* regenerative processes resulting from the effect of experimental samples of synthetic polyvinyl formal based hydrogel implants**

Samchenko Yu.M. ¹, Maletskiy A.P. ², Dybkova S.M. ¹, Gruzina T.G. ¹,
Rieznichenko L.S. ¹, Podolska V.I. ¹, Kernosenko L.O. ¹, Artemov O.V. ², Poltoratska T.P. ¹,
Zholobak N.M. ³, Kolesnichenko V.G. ⁴

¹F.D. Ovcharenko Institute of Biocolloidal Chemistry, National Academy of Sciences of Ukraine

Kyiv (Ukraine)

²SI "The Filatov Institute of Eye Diseases and Tissue Therapy of the National Academy of Medical Sciences of Ukraine"

Odesa (Ukraine)

³Zabolotny Institute of Microbiology and Virology, National Academy of Sciences of Ukraine

Kyiv (Ukraine)

⁴Frantsevich Institute for Problems of Materials Science, National Academy of Sciences of Ukraine

Kyiv (Ukraine)

Key words:

PVF, hydrogel implants, orbit, regeneration, *in vitro*, *in vivo*, biocompatibility, implantation

Purpose: To experimentally examine *in vitro* and *in vivo* regenerative processes resulting from the effect of experimental samples of synthetic (poly)vinyl formal (PVF) based hydrogel implants.

Material and Methods: Scanning electron microscopy (SEM) analysis; Vero cell culture evaluation of *in vitro* regenerative processes by the wound-healing assay; evaluation of *in vivo* regenerative processes in the rabbit ocular and crest tissues resulting from the effect of experimental samples of synthetic PVF based hydrogel implants. Experimental studies of hybrid hydrogels were conducted in 20 Chinchilla rabbits (age, 5–6 months and weight, 2–3 kg) that were maintained and fed under similar conditions.

Results: The most active regeneration of the damaged Vero cell monolayer (with a wound closure percentage of 91%) resulted from the effect of the sample of PVF/AuNP (12.06 µg/g) hydrogel, followed by PVF-based hydrogel and PVF-based hydrogel impregnated with poly(N-isopropylacrylamide) (PNIPAM). In an *in vivo* study of local effects after implantation of PVF/AuNP (12.06 µg/g) hydrogel in the scleral sac, orbital tissue or below the crest intradermally, the rabbits who underwent this implantation exhibited mild edema of postoperative suture site and adjacent conjunctiva which reduced on day 10 and practically disappeared on days 17–19. Histomorphological studies of responses of the rabbit orbital and crest tissue to the hydrogel implant found neither implant resorption nor acute inflammation of the surrounding tissue.

Conclusion: Our *in vitro* and *in vivo* study of regenerative processes resulting from the effect of experimental samples of synthetic PVF based hydrogel implants demonstrated that PVF/AuNP (12.06 µg/g) hydrogel is highly biocompatible and had promise as an implant material.

Introduction

A study on facial and penetrating neck injuries sustained in combat operations in Iraq and Afghanistan from 2011 to 2016 [1] found that the most common facial fractures were of the orbit (26.3%) and maxilla/zygoma (25.1%).

In recent years there has been a significant increase in the number of patients who suffered from combat actions in Ukraine. Combat injuries to the eye are characterized by substantial damage to ocular tissues and socket and multiple fragmentation wounds, which are frequently concomitant with injuries to the face and other body parts.

Given a rising tendency in the rate of ocular trauma, there is an increasing need in surgeries for orbital and periorbital reconstruction.

The ocular surgeon has to use implant materials to (1) replace soft tissue and bone structures during orbital and periorbital reconstructive surgeries and (2) shape a musculoskeletal stump to improve prosthesis position in

© Samchenko Yu.M., Maletskiy A.P., Dybkova S.M., Gruzina T.G., Rieznichenko L.S., Podolska V.I., Kernosenko L.O., Artemov O.V., Poltoratska T.P., Zholobak N.M., Kolesnichenko V.G., 2025

the frontal plane and its motility, thus contributing to improved cosmetic outcome of enucleation or evisceration. A disadvantage of biological (autologous and homologous) implant materials is that they tend to have problems with resorption. In recent decades, inorganic and synthetic materials have been intensively developed to overcome the drawbacks of autologous and homologous implant materials [2]. Clinical studies, however, demonstrated that these materials are inadequately biocompatible and do not ensure intergrowth of biological tissue in any of them.

Therefore, it is important to develop advanced synthetic materials for orbital and facial bone reconstruction and filling postoperative cavities. Non-biological implants with a porous structure (first and foremost, cross-linked hybrid gels) capable of biological integration with the adjacent orbital tissue provide new opportunities to perform restorative surgery. A hybrid hydrogel-based polymeric material may be a promising material for these applications. Due to their structural similarity to the hydrated macromolecular components of the body, polymeric hydrogels occupy a special place among today's implant materials [3]. However, conventional hydrogels have a few shortcomings (poor mechanical strength, insufficient biocompatibility, and no biological activity, e.g., little or no capacity to stimulate adhesion and growth of eukaryotic cells) that limit their application as implant materials [4]. Additionally, drug diffusion from conventional hydrogels is insufficiently controllable, insufficiently targeted at a specific organ, and insufficiently prolonged. Therefore, not conventional but smart hydrogels have been increasingly used recently. They can respond to relatively small changes in external stimuli (mainly, physiological temperature and pH changes) with phase transition and rapid changes in their physical and chemical parameters (e.g., degree of swelling and porosity, sorption and diffusion characteristics). Using smart hydrogels in drug delivery systems can reduce the dosing frequency, maintain the desired therapeutic concentration in a single dose, and minimize the drugs' side effects by preventing the accumulation of the drugs in non-target tissues [5]. The most studied gels of this class are polyacrylic acid-based pH-sensitive hydrogels [6] and hydrogels based on thermosensitive polymers such as poly(N-isopropylacrylamide) (PNIPAM) [7]. Cross-linked PNIPAM-based hydrogels demonstrate desolvation at a higher temperature than their lower critical solution temperature (LCST) of 32.8 °C which is close to the human body temperature [8] due to the balance between hydrophilic (water-polymer) and hydrophobic (polymer-polymer) interactions. This temperature can be precisely controlled through copolymerization with other monomers, aiming at controlled release at the tumor site of therapeutics from thermoresponsive nanogels [9].

The development of composite hydrogels with incorporated metallic nanoparticles has become a new area of research in tissue engineering and regenerative medicine. Overall, the mechanical, physical, and biological properties of nanocomposite hydrogels will vary depending on

the synthesis strategy, nanomaterial choice, and network formation approach. By optimizing these parameters (individually or in synchrony) tailored applications such as custom release profiles of bioactive cues, cell viability, spreading, and scaffold infiltration can be achieved [10-12].

The unique physical and chemical properties of gold nanoparticles (AuNPs) depend on their size and shape, making them the perfect choice for nanomaterial composite hydrogels for a variety of biomedical applications. AuNPs have been widely used in developing approaches to the treatment of cancer (photothermal and photodynamic treatment), as a substance with antiangiogenic properties, vectors for targeted delivery of anti-tumor agents, etc [13, 14].

Anti-inflammatory and antioxidative properties of AuNPs deserve special attention [15]. Of particular importance is their capacity to induce cell adhesion on hydrogel surface [16] and stimulate tissue regeneration [17]. Other considerable advantages of composite hybrid hydrogels with AuNPs are their high biocompatibility and low irritation to the skin and/or eyes [12]. The above biological properties of AuNPs make them widely used in designing nanocomposite hybrid hydrogels with tailored characteristics [18-21].

The purpose of the study was to experimentally examine *in vitro* and *in vivo* regenerative processes resulting from the effect of experimental samples of synthetic polyvinyl formal (PVF) based hydrogel implants.

Material and Methods

Synthesis of experimental samples of synthetic PVF based hydrogel implants has been previously described by us [22, 23]; these samples are shown in Fig. 1.

Morphology and structure of experimental samples of synthesized PVF based hydrogel implants were examined by scanning electron microscopy (SEM) using a TESCAN MIRA 3 LMU device with an energy dispersive spectrometer (EDS, Oxford Max-80) and a precision etching coating system (PECS, Gatan 682).

Thermogravimetric analysis (TGA) and differential thermogravimetry (DTG) were employed to assess the properties of PVF based hydrogels filled with PNIPAM.

In vitro regenerative processes resulting from the effect of experimental samples of PVF based hydrogels were examined using the *in vitro* scratch assay, a common technique allowing the observation of two-dimensional cell migration and proliferation during regenerative processes [24]. The inoculated monolayer Vero cell culture from the Cell culture collection of the Zabolotny Institute of Microbiology and Virology was used as a test culture. Cells were plated on 6 well plates at a density of 1×10^5 cell/ml and grown in Dulbecco's Modified Eagle Medium/Nutrient Mixture F-12 (DMEM/F12) containing 10% fetal bovine serum (FBS) with antibiotic-antimycotic at 37 °C with 5% CO₂.

Twenty four hours after cell plating, monolayer cell cultures were wounded with a 1-ml sterile pipette tip.

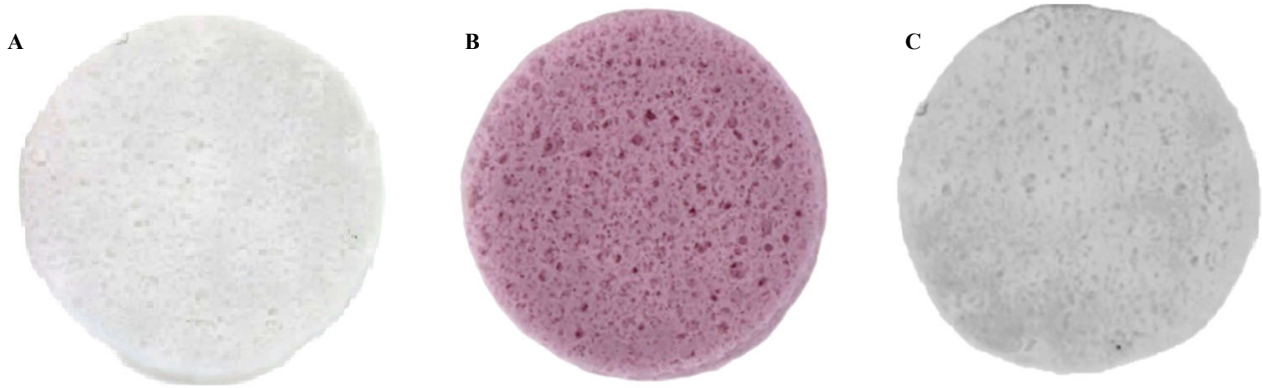


Fig. 1. Photographs of experimental samples of synthetic polyvinyl formal (PVF) based hydrogel implants: PVF hydrogel (alias, PVF-based hydrogel) (A); PVF/AuNP hydrogel (PVF based hydrogel with incorporated gold nanoparticles) (B); PVF-based PNIPAM hydrogel (polyvinyl formal based hydrogel impregnated with poly(N-isopropylacrylamide) (C)

Thereafter, the medium was replaced with a native medium in test wells and samples of conditioned media. The medium was conditioned with hydrogel samples via their extraction by the medium at 37 °C for 24 hours as per the standard [25].

In 48 hours, the efficacy of scratch wound closure was assessed by crystal violet cell staining and open source image J/Fiji software and the Wound_healing_size_tool plug-in [26].

The wound closure percentage (WCP) was determined using the following formula:

$$WCP = ((W_{t_0} - W_{\Delta t}) / W_{t_0}) \times 100\%$$

where W_{t_0} is the average scratch width at the t_0 time point and

$W_{\Delta t}$ is the average scratch width at the Δt time point (48 hours).

In vivo response to PVF based hydrogels was examined through the analysis of changes in clinical and pathomorphological parameters in 20 Chinchilla rabbits (age, 5–6 months and weight, 2–3 kg) from the vivarium of SI “The Filatov Institute of Eye Diseases and Tissue Therapy of the National Academy of Medical Sciences of Ukraine”.

All animal experiments were performed in compliance with the principles of European Convention for the Protection of Vertebrate Animals Used for Experimental and Other Scientific Purposes from the European Treaty Series (Strasbourg, 1986), First National Bioethics Congress (Kyiv, 2021), and Law of Ukraine on Protection of Animals from Cruel Treatment No. 3447-IV dated 21.02.2006, and approved by a local Bioethics Committee of SI “The Filatov Institute of Eye Diseases and Tissue Therapy of the National Academy of Medical Sciences of Ukraine” (Committee Minutes dated 20.04.2024). Prior to surgical procedure, animals were anesthetized with thiopental sodium 0.1% (1.0 mL/kg, intramuscularly).

To investigate the soft tissue response in rabbits, hybrid hydrogel samples (PVF/AuNP hydrogel; 12.06 µg/g; size, 10.0 x 10.0 x 2.5 mm) were placed in the scleral sac

(5 animals), orbital tissue (5 animals), or below the crest intradermally (10 animals).

A PVF based hybrid hydrogel implant with incorporated AuNPs (12.06 µg/g) was placed either in the scleral sac after evisceration or below the crest intradermally after skin incision. The wound was closed with interrupted 6-0 silk sutures.

Clinical signs (edema of the orbital tissue, edema of the cheek, state of sutures, presence of discharge) were scored on days 2, 5, 10 and 30 and every 5 days thereafter until the end of the study as follows:

1) Edema of orbit tissue (0, no edema; 1, edema of postoperative suture site; 2, edema of postoperative suture site and adjacent conjunctiva; and 3, marked conjunctival chemosis and edema of the soft orbital tissue)

2) State of sutures (0, no suture line disruption; 1, solitary sites of suture line disruption, up to 1.0 mm; 2, sites of suture line disruption, 1.0-5.0 mm; and 3, disruption along the entire suture length) and

3) Conjunctival discharge (0, no discharge; 1, mild sanious discharge from the conjunctiva and at eyelid margins; 2, mild sanious and serous discharge from the conjunctival sac, at eyelid margins, and at the orbital area; and 3, marked sanious and serous discharge from the conjunctival sac, at eyelid margins, and both at orbital area and outside the orbit).

Implants were cut out with the surrounding tissue for immediate histomorphological examination at days 10 and 30. Animals were euthanized by air embolism under general anesthesia with thiopental sodium 0.1% (1.0 mL/kg body weight, intramuscularly). Tissue samples were fixed in 10% formalin for 24 hours and then embedded in paraffin. Formalin-fixed, paraffin-embedded histological tissue sections were stained with hematoxylin and eosin and examined using a microscope (Jenamed 2; Carl Zeiss, Jena, Germany) at magnifications x100 to x400.

Microsoft Excel software (Microsoft) was used for calculations. Data are presented as mean \pm standard error of mean.

Results

Scanning electron microscopy (SEM) showed that PVF matrices had a hierarchical porous structure with large interconnected transport pores (with a Feret diameter of 100–200 μm) and significantly smaller pores (about 5–10 μm) in their walls (Fig. 2a). Pores formed a homogeneous honeycomb structure with 1- μm -thick walls. The inclusion

of AuNPs at a concentration of 12.06 $\mu\text{g/g}$ (i.e., a gold to PVF ratio of 1:100000) did not change the architecture of the PVF matrix (Fig. 2b), because the distribution, shape and size of pores did not change. This indicates that AuNPs can be introduced in the PVF matrix with no impact on the porous structure of the matrix. Filling the matrix with PVF based PNIPAM hydrogel resulted in a significant decrease in the size of macropores and increase in the size of pore walls to 2–3 μm (Fig. 2c), with no blockage of transport pores.

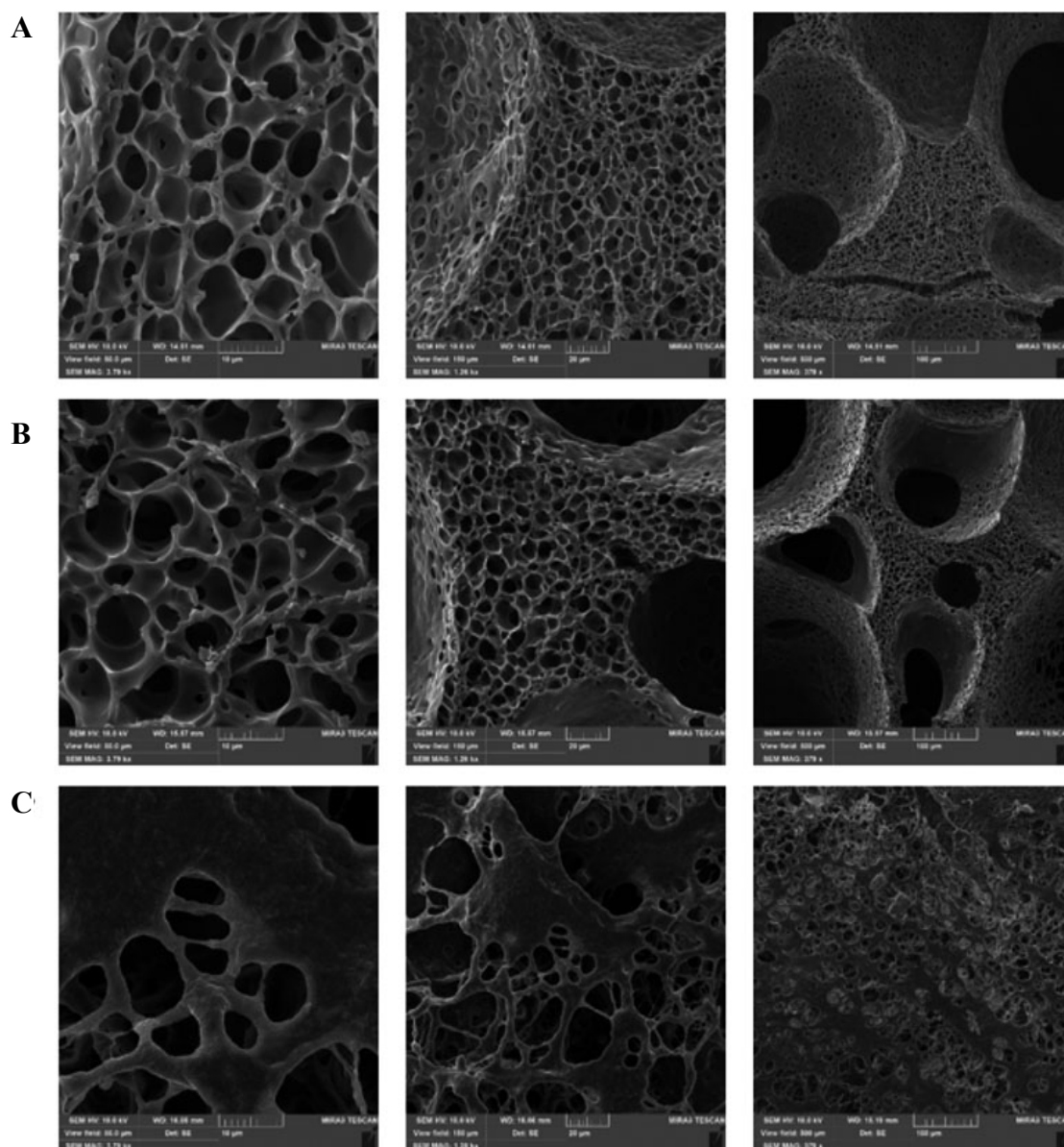


Fig. 2. Scanning electron microscopy (SEM) photographs of polyvinyl formal (PVF) hydrogel (A); PVF based hydrogel with incorporated gold nanoparticles (PVF/AuNP hydrogel, 12.06 $\mu\text{g/g}$) (B); polyvinyl formal based hydrogel impregnated with poly(N-isopropylacrylamide) (PVF-based PNIPAM hydrogel) (C). Original magnifications: x 3790 (A); x 1290 (B); x 379 (C)

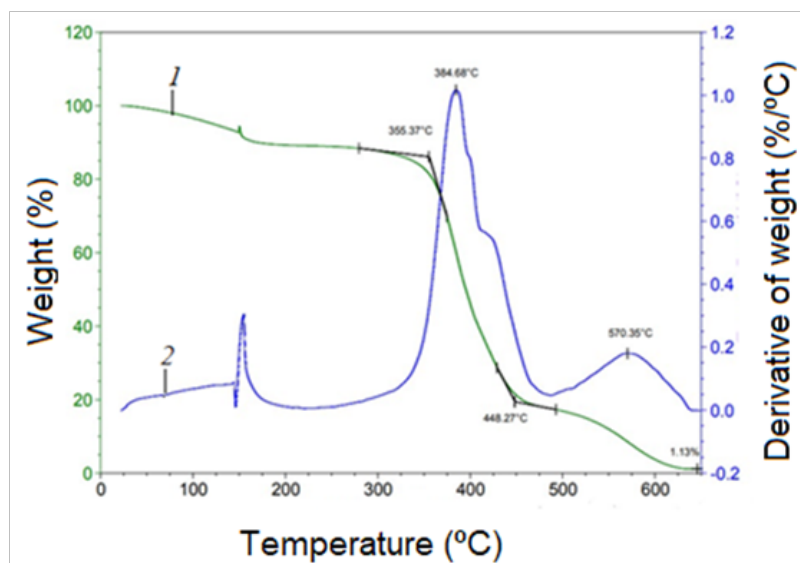


Fig. 3. Thermogravimetric analysis (1) and differential thermogravimetry (2) curves for polyvinyl formal based hydrogel impregnated with poly(N-isopropylacrylamide)

The results of TGA provided a comprehensive understanding of the behavior of PVF based PNIPAM hydrogel at different thermal conditions (Fig. 3). We found that heating at a temperature ranging from 20 to 150 °C resulted in insubstantial (about 5%) loss of weight due to evaporation of both volumetric water and the water adsorbed by the functional groups of the polymer. A wide plateau region extending to 300 °C was attained further on, indicating the absence of destructive processes at this temperature range.

A weight loss with a further increase in temperature was associated with a release of volatile components by the present functional groups during their thermolysis, which was clearly seen on the DTG curve at a maximum of 385 °C. These volatile components were mainly NH_3 , CO and CO_2 of the amide group present in PNIPAM. Further heating resulted in fragmentation of the hydrocarbon skeleton at 450 °C and dehydroxylation of residual hy-

droxyl groups and complete destruction and combustion of organic macromolecules at 530 °C.

Therefore, the synthesized hydrogels exhibited good thermal stability within a temperature range significantly greater than that in which they are usually used. Additionally, they withstand steam sterilization at 121 °C for 15 minutes without substantial changes, which is extremely important for medical devices.

Table 1 and Figure 4 present the results of evaluation of in vitro and in vivo regenerative processes resulting from the effect of experimental samples of PVF based hydrogels.

The most active regeneration of the damaged Vero cell monolayer resulted from the effect of the sample of PVF/AuNP (12.06 $\mu\text{g/g}$) hydrogel. The mean WCP for this sample was which significantly better than for the monolayer of control cells (91% versus 60%, respectively).

Table 1. Efficacy of in vitro regeneration of Vero cells resulting from the effect of synthesized hydrogels

Sample	W_{t_0} (pixel), wound width at baseline (t_0) $M \pm m$	$W^{\Delta t}$ (pixel), wound width in 48 hours (Δt) $M \pm m$	Wound closure percentage
Control	868.21 \pm 9.10	351.18 \pm 48.99	60
PVF/AuNP hydrogel (12.06 $\mu\text{g/g}$)	868.21 \pm 9.10	74.86 \pm 41.05	91
PVF hydrogel	868.21 \pm 9.10	183.65 \pm 44.23	79
PVF-based PNIPAM hydrogel	868.21 \pm 9.10	212.77 \pm 49.18	76

Note: PVF hydrogel, polyvinyl formal based hydrogel; PVF/AuNP hydrogel (12.06 $\mu\text{g/g}$), polyvinyl formal based hydrogel with incorporated gold nanoparticles; PVF-based PNIPAM hydrogel, polyvinyl formal based hydrogel impregnated with poly(N-isopropylacrylamide)

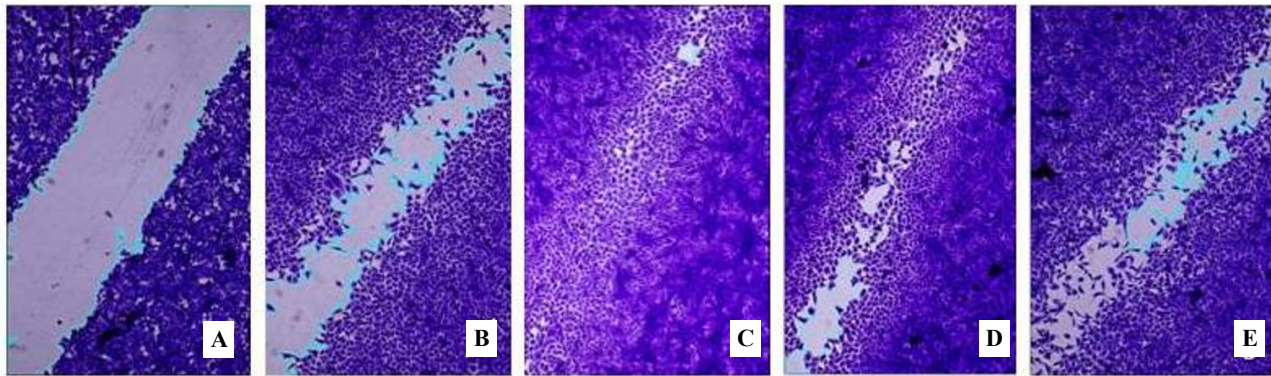


Fig. 4. Regeneration of Vero cell monolayer. Wound width at baseline (time point t_0) (A). Efficacy of wound closure in 48 hours (time point $t_{\Delta t}$) in control (B) and the medium conditioned with polyvinyl formal based hydrogel with incorporated gold nanoparticles (PVF/AuNP hydrogel, 12.06 $\mu\text{g/g}$) (C), polyvinyl formal based hydrogel (PVF hydrogel) (D), and polyvinyl formal based hydrogel impregnated with poly(N-isopropylacrylamide) (PVF-based PNIPAM hydrogel) (E)

Forty-eight hours after wound infliction, just signs of the formation of areas of complete wound confluence (Fig. 4b) in controls, and areas of complete confluence in the cell monolayer were observed in the media conditioned with the sample of PVF/AuNP (12.06 $\mu\text{g/g}$) hydrogel (Fig. 4c).

The mean WCP for the sample of PVF hydrogel was smaller than for the sample of PVF/AuNP (12.06 $\mu\text{g/g}$) hydrogel (79% versus 91%), but was 19% larger than for controls (60%). Good cell growth with the formation of confluence areas was seen at the site of scratch (Fig. 4d).

Forty-eight hours after wound infliction, formation of areas of complete wound confluence of the damaged Vero cell monolayer, with a mean WCP of 76%, was observed for the sample of PVF-based hydrogel impregnated with PNIPAM (Fig. 4e). Therefore, in the media conditioned with the sample of PVF-based hydrogel impregnated with PNIPAM, the efficiency of regeneration of the damaged Vero cell monolayer as assessed by the WCP was rather close to that in the media conditioned with the sample of PVF-based hydrogel.



Fig. 5. State of the orbital tissue on day 5 after implantation of polyvinyl formal based hydrogel with incorporated gold nanoparticles (PVF/AuNP hydrogel, 12.06 $\mu\text{g/g}$) in this tissue

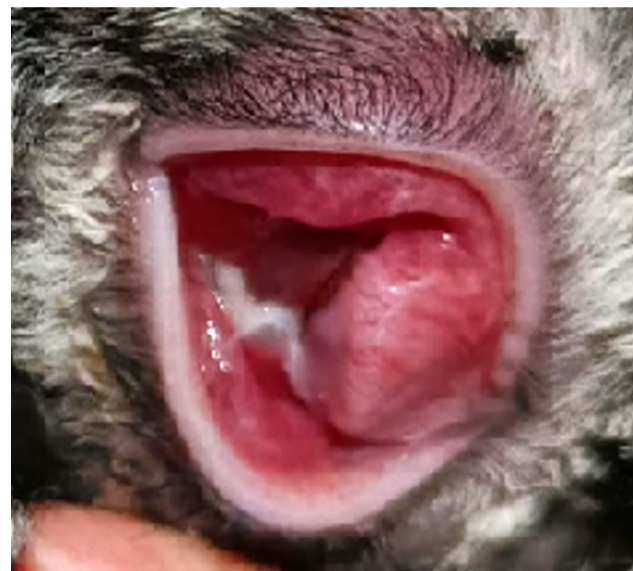


Fig. 6. State of the orbital and conjunctival tissue on day 5 after implantation of polyvinyl formal based hydrogel with incorporated gold nanoparticles (PVF/AuNP hydrogel, 12.06 $\mu\text{g/g}$) in the scleral sac



Fig. 7. State of the crest skin tissue on days 5 (A) and 10 (B) after implantation of polyvinyl formal based hydrogel with incorporated gold nanoparticles (PVF/AuNP hy-drogel, 12.06 $\mu\text{g/g}$)

Given the efficacy of regenerative processes resulting from the effect of experimental samples of PVF based hydrogels, the sample of PVF/AuNP (12.06 $\mu\text{g/g}$) hydrogel was selected for subsequent *in vivo* experiments.

On days 5 to 10 after implantation of PVF/AuNP (12.06 $\mu\text{g/g}$) hydrogel in the orbital tissue, all animals who underwent this implantation exhibited edema of postoperative suture site and adjacent conjunctiva (Fig. 5).

On day 10, there was mild conjunctival edema, wound edges appeared well approximated, and sutures were still in place.

On days 1 to 5 after implantation of PVF/AuNP (12.06 $\mu\text{g/g}$) hydrogel in the scleral sac, all animals who under-

went this implantation exhibited conjunctival and orbital edema, with sutures still being in place (Fig. 6).

Additionally, on days 5 to 10, sanious and serous discharge from the conjunctival sac was observed.

Observation of the postoperative wound of the skin and conjunctiva on days 2, 5 and 10 revealed that wound healing was by primary intention.

After implantation of PVF/AuNP (12.06 $\mu\text{g/g}$) hydrogel below the crest intradermally, mild tissue edema at the site of implantation was observed on day 5 (Fig. 7a), and was found to be absent on day 10 (Fig. 7b).

Histological studies of *in vivo* soft tissue response on days 10 to 30 after implantation of PVF/AuNP (12.06

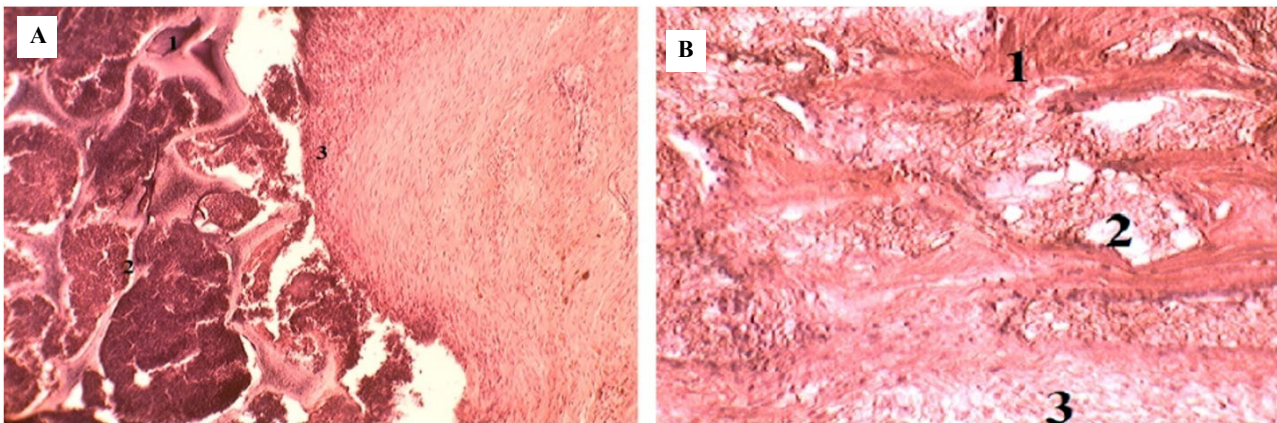


Fig. 8. Polyvinyl formal based hydrogel with incorporated gold nanoparticles (PVF/AuNP hydrogel, 12.06 $\mu\text{g/g}$) on days 10 (1, residual implant; 2, accumulation of macrophages /histiocytes); 3, dense fibrous tissue) (A) and 30 (1, fibroblast proliferation; network structure; 3, fibrous tissue) (B) after placement in the orbital tissue. Original magnification: 100x

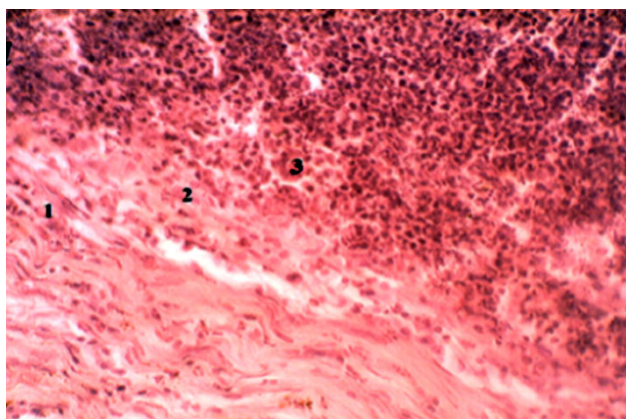


Fig. 9. Polyvinyl formal based hydrogel with incorporated gold nanoparticles (PVF/AuNP hydrogel, 12.06 µg/g) on day 10 (1, fibrous tissue; 2, fibroblast proliferation; 3, accumulation of macrophages/ histiocytes) (A) after placement in the scleral sac. Original magnification: 200x

µg/g) hydrogel showed that, in tissues adjacent to the implant, inflammatory changes were mild, with mainly small lymphocyte infiltrates and sometimes eosinophilic infiltrates, without foci of suppurative inflammation (infiltration of white blood cells). On days 10 to 30, we noted a tendency toward implant replacement with fibrous connective tissue. However, the process of implant replacement did not complete: in all cases, sites of macrophage/histiocyte infiltration or mild fibroblast infiltration and implant fragments remained at the edge of the implant. These sites were seen as areas of intense hematoxylin staining (basophilic sites) or eosinophilia, sometimes with inclusions of network structures.

On day 10 after implantation, the percentage ratio of the residual to the total area of the implant ranged from 30 to 50%.

There were macrophage/histiocyte infiltrates with peripheral displacement of histiocytes (macrophages) by fibroblastic cells that exhibited migration to the fibrous tissue at the margin between the implant and surrounding dense fibrous tissue.

On day 30 after implantation, fibrous tissue could be seen also in deep layers of the implant. Nevertheless, until this time point, the percentage of the total implant area replaced by fibrous tissue did not exceed 50–70%, with occasional sites of macrophage/histiocyte infiltrates showing signs of fibroblast proliferation. Gradual development of fibrous tissue resulted in macrophage/histiocyte displacement from the periphery to the center of the implant.

No implant resorption was observed; rather the site of hydrogel implantation was presented by macrophages/histiocytes, fibroblasts and fibrous tissue. Figs. 8 and 9 show the examples of major histopathological patterns of changes in the implant on days 10 and 30.

Histologically, implants were seen as chaotically distributed areas of amorphous hematoxylin-and-eosin staining, sometimes with insignificant involvement of non-stained filamentous cells, likely due to the presence of corresponding basophilic and acidophilic groups in the polymer structure. Until day 30 after implantation of PVF/AuNP (12.06 µg/g) hydrogel into the sclera sac, orbital tissue or intradermally, the above cells were occasionally present, accounting for 5-10% of the total area of the histological section of the implant.

Discussion

Our energy-dispersive X-ray (EDX) analysis of hydrogels showed that C and O were the major elements present in the PVF-based hydrogel, PVF/AuNP hydrogel and PVF-based hydrogel impregnated with PNIPAM, but only the latter hydrogel contained also nitrogen. In addition, this nitrogen was homogeneously distributed (mean and standard deviation for percentage content of nitrogen, $11.61 \pm 0.51\%$), indicating the homogeneity of this hydrogel. The hierarchical porous structure of PVF matrices can provide an ideal environment for cell growth and nutrient transport, potentially enhancing the effectiveness of applications of PVF nanocomposites in tissue engineering and plastic and reconstructive surgery. However, understanding the thermal behavior of PVF-based implants is also important. The key features (like phase transitions, thermal stability and decomposition temperature) have a direct impact on durability and applicability of PVF-based hybrid hydrogels in tissue engineering and medicine.

The wound-healing assay is commonly used today for evaluating *in vitro* regenerative processes. It simulates cell migration *in vivo* [27], is simple, inexpensive, and does not require the use of special cultures of eukaryotic cells.

In the current study, the wound-healing assay was used for evaluating the effect of synthesized PVF-based hydrogels on *in vitro* regeneration of the damaged Vero cell monolayer. The most active regeneration of the damaged Vero cell monolayer resulted from the effect of the sample of PVF/AuNP (12.06 µg/g) hydrogel, followed by PVF-based hydrogel and PVF-based hydrogel impregnated with PNIPAM. An increased regenerative potential of PVF/AuNP (12.06 µg/g) hydrogel compared to PVF-based hydrogel is likely to be caused by the effect of AuNPs, which is confirmed by the literature [12].

In vivo studies of regenerative processes demonstrated that, on days 1 to 5 after implantation of PVF/AuNP (12.06 µg/g) hydrogel in the sclera sac, orbital tissue or below the crest intradermally, all rabbits who underwent this implantation exhibited edema of postoperative suture and adjacent conjunctiva and mild serous and serous discharge from the conjunctival sac. These edema and discharge reduced after 5 days and disappeared on days 8-10.

Histomorphological studies showed PVF/AuNP (12.06 µg/g) hydrogel had good biocompatibility and did not cause a negative inflammatory response in the form of acute inflammation. The inflammatory reactions seen in the tissues adjacent to the implant included mostly mild

diffuse lymphocytic infiltration close to the implant surface, with no inflammatory reactions seen at the sites more remote from the implant. Most frequently, inflammatory reaction was seen on day 10, tending to reduce on day 30.

PVF/AuNP (12.06 µg/g) implant staying in the scleral sac, orbital tissue or below the crest intradermally resulted in gradual implant replacement with fibrous connective tissue. Additionally, no macrophage reaction (e.g., no multinuclear giant cell reaction) was observed, evidencing against implant resorption.

Conclusion

Therefore, the most active *in vitro* regeneration of the damaged Vero cell monolayer resulted from the effect of the sample of PVF/AuNP (12.06 µg/g) hydrogel, the mean WCP for this sample (91%) being significantly superior to those of examined samples of other hydrogels. *In vivo* studies of local effects demonstrated that, after implantation of PVF/AuNP (12.06 µg/g) hydrogel in the scleral sac, orbital tissue or below the crest intradermally, the rabbits exhibited mild edema of postoperative suture and adjacent conjunctiva, which soon resolved.

Histomorphological studies of responses of the rabbit orbital and crest tissue to the hydrogel implant found neither implant resorption nor acute inflammation of the surrounding tissue.

Our *in vitro* and *in vivo* study of regenerative processes resulting from the effect of experimental samples of synthetic PVF based hydrogel implants demonstrated that PVF/AuNP (12.06 µg/g) hydrogel is highly biocompatible and had promise as an implant material.

References

- Lanigan A, Lindsey B, Maturo S, Brennan J, Laury A. "The Joint Facial and Invasive Neck Trauma (J-FAINT) Project, Iraq and Afghanistan: 2011-2016. *Otolaryngol Head Neck Surg.* 2017 Oct;157(4):602-607. doi: 10.1177/0194599817725713.
- Bordbar-Khiabani A, Gasik M. Smart hydrogels for advanced drug delivery systems. *Int J Mol Sci.* 2022 Mar 27;23(7):3665. doi: 10.3390/ijms23073665.
- Clasky AJ, Watchorn JD, Chen PZ, Gu FX. From prevention to diagnosis and treatment: Biomedical applications of metal nanoparticle-hydrogel composites. *Acta Biomater.* 2021 Mar 1;122:1-25. doi: 10.1016/j.actbio.2020.12.030.
- Chugh H, Sood D, Chandra I, Tomar V, Dhawan G, Chandra R. Role of gold and silver nanoparticles in cancer nano-medicine. *Artif Cells Nanomed Biotechnol.* 2018;46(sup1):1210-1220. doi: 10.1080/21691401.2018.1449118.
- Crezee J, Franken NAP, Oei AL. Hyperthermia-based anti-cancer treatments. *Cancers (Basel).* 2021 Mar 12;13(6):1240. doi: 10.3390/cancers13061240.
- Darweesh RS, Ayoub NM, Nazzal S. Gold nanoparticles and angiogenesis: molecular mechanisms and biomedical applications. *Int J Nanomedicine.* 2019 Sep 19;14:7643-7663. doi: 10.2147/IJN.S223941.
- Grant SA, Zhu J, Gootee J, Snider CL, Bellrichard M, Grant DA. Gold Nanoparticle-Collagen Gels for Soft Tissue Augmentation. *Tissue Eng Part A.* 2018 Jul;24(13-14):1091-1098. doi: 10.1089/ten.TEA.2017.0385.
- Habib LA, Yoon MK. Patient specific implants in orbital reconstruction: A pilot study. *Am J Ophthalmol Case Rep.* 2021 Oct 19;24:101222. doi: 10.1016/j.ajoc.2021.101222. PMID: 34746511; PMCID: PMC8554165
- Heo DN, Ko WK, Bae MS, Lee JB, Lee DW, Byun W, et al. Enhanced bone regeneration with a gold nanoparticle-hydrogel complex. *J Mater Chem B.* 2014; 2, 1584-1593. doi: 10.1039/c3tb21246g.
- Ho TC, Chang CC, Chan HP, Chung TW, Shu CW, Chuang KP, et al. Hydrogels: Properties and applications in biomedicine. *Molecules.* 2022 May 2;27(9):2902. doi: 10.3390/molecules27092902.
- ISO 10993-12, ISO 10993-12:2012 Biological evaluation of medical devices — Part 12: Sample preparation and reference materials, 2014 (2014).
- Jafari M, Paknejad Z, Rad MR, Motamedian SR, Eghbal MJ, Nadjmi N, et al. Polymeric scaffolds in tissue engineering: a literature review. *J Biomed Mater Res B Appl Biomater.* 2017 Feb;105(2):431-459. doi: 10.1002/jbm.b.33547.
- Kim B, Lee JS. Thermally reversible shape transformation of nano-patterned PNIPAAm hydrogel. *Polym Bull.* 2021;78: 3353–3361. doi:10.1007/s00289-020-03276-3.
- Li H, Pan S, Xia P, Chang Y, Fu C, Kong W, et al. Advances in the application of gold nanoparticles in bone tissue engineering. *J Biol Eng.* 2020 May 6;14:14. doi: 10.1186/s13036-020-00236-3.
- Lee D, Heo DN, Nah HR, Lee SJ, Ko WK, Lee JS, et al. Injectable hydrogel composite containing modified gold nanoparticles: implication in bone tissue regeneration. *Int J Nanomedicine.* 2018 Nov 1;13:7019-7031. doi: 10.2147/IJN.S185715.
- Liang CC, Park AY, Guan JL. In vitro scratch assay: a convenient and inexpensive method for analysis of cell migration in vitro. *Nat Protoc.* 2007;2(2):329-33. doi: 10.1038/nprot.2007.30.
- Memic A, Alhadrami HA, Hussain MA, Aldahiri M, Al Nowaiser F, Al-Hazmi F, et al. Hydrogels 2.0: improved properties with nanomaterial composites for biomedical applications. *Biomed Mater.* 2015 Dec 23;11(1):014104. doi: 10.1088/1748-6041/11/1/014104.
- Pinho RA, Hauptenthal DPS, Fauser PE, Thirupathi A, Silveira PCL. Gold nanoparticle-based therapy for muscle inflammation and oxidative stress. *J Inflamm Res.* 2022 May 31;15:3219-3234. doi: 10.2147/JIR.S327292.
- Ratemi E. 5-pH-responsive polymers for drug delivery applications. In: Makhlof ASH, Abu-Thabit NY, editors. *Woodhead publishing series in biomaterials, stimuli responsive polymeric nanocarriers for drug delivery applications, V.1.* Woodhead Publishing; 2018. p.121-141. doi: 10.1016/B978-0-08-101997-9.00005-9.
- Rodriguez LG, Wu X, Guan JL. Wound-healing assay. *Methods Mol Biol.* 2005;294:23-9. doi: 10.1385/1-59259-860-9:023.
- Samchenko YuM, Dybkova SM, Maletskyi AP, Kernosenko LO, Artiomov OV, Gruzina TG, et al. In vitro and in vivo study of the biocompatibility and adjacent soft tissue response to synthetic polyvinylformal hydrogel implant. *Oftalmol Zh.* 2024; 110:45–51. doi: 10.31288/oftalmolzh202434551.
- Samchenko YuM, Dybkova SM, Reznichenko LS, Kernosenko LO, Gruzina TG, Poltoratska TP, et al. Synthesis and study on antimicrobial properties of hydrogel materials for maxillo-facial Surgery. *Him Fiz Tehnol Poverhni.* 2024;15:110–118. doi:10.15407/hftp15.01.110.
- Suarez-Arnedo A, Torres Figueroa F, Clavijo C, Arbeláez P, Cruz JC, Muñoz-Camargo C. An image J plugin for the high throughput image analysis of in vitro scratch wound healing assays. *PLoS One.* 2020 Jul 28;15(7):e0232565. doi: 10.1371/journal.pone.0232565.
- Tan HL, Teow SY, Pushpamalar J. Application of metal nanoparticle-hydrogel composites in tissue regeneration. *Bioengineering.* 2019; 6(1):17. doi: 10.3390/bioengineering6010017.

Disclosures

Received: 07.04.2025

Accepted: 08.06.2025

Corresponding author: *Anatolii P. Maletskiy, SI "The Filatov Institute of Eye Diseases and Tissue Therapy of the National Academy of Medical Sciences of Ukraine", Odesa (Ukraine), 49/51 Frantsuzkyi Bulvar, Odesa, 65015, Ukraine*

Author's contribution. YuMS: Conceptualization and Design of the Study, Literature Data Collection and Analysis, Writing-original draft, Writing-review & editing; APM: Conceptualization and Design of the Study; SMD: Conceptualization and Design of the Study, Evaluation of *in vitro* and *in vivo* Regenerative Potential of Hydrogel Implant Samples; TGG, LSR, VIP: Evaluation of *in vitro* and *in vivo* Regenerative Potential of Hydrogel Implant Samples; LOK, TPP: Hydrogel Synthesis and Characterization; OVA: Histological Studies; NMZh: Cultivation of Vero Cells, Evaluation of *in vitro* and *in vivo* Regenerative Potential of Hydrogel Implant Samples; VGK: Hydrogel Thermostability Studies, Thermogram Interpretation. All authors reviewed the results and approved the final version of the manuscript.

Funding: *This study was conducted within the framework of Science for Safety and Sustainable Development of Ukraine Call for Projects launched by the National Research Foundation of Ukraine (Project Identification Number, 2021.01/0178)*

Conflict of interest: *The authors certify that they have NO affiliations with or involvement in any organization or entity with any financial interest or non-financial interest in the subject matter or material discussed in this manuscript.*

Abbreviations: AuNP, gold nanoparticles; DSC, differential scanning calorimetry; DTG, differential thermogravimetry; LCST, lower critical solution temperature; PNIPAM, poly (N-isopropylacrylamide); PVA, polyvinyl alcohol; PVF, (poly)vinyl formal; PVF hydrogel, (poly) vinyl formal based hydrogel; PVF/AuNP hydrogel, (poly) vinyl formal based hydrogel with incorporated gold nanoparticles; PVF-based PNIPAM hydrogel, (poly)vinyl formal based hydrogel impregnated with poly(N-isopropylacrylamide); SEM, scanning electron microscopy; TGA, thermogravimetric analysis